12-2006

ASSEMBLY AND MODIFICATION OF A HYPERTHERMAL AND LOW ENERGY ION BEAMLINE FOR DETECTING ELECTRON-HOLE PAIR PRODUCTION IN SCHOTTKY DIODES

Matthew Ray
Clemson University, mpray@clemson.edu

ASSEMBLY AND MODIFICATION OF A HYPERTHERMAL AND LOW ENERGY ION BEAMLINE FOR DETECTING ELECTRON-HOLE PAIR PRODUCTION IN SCHOTTKY DIODES

A Thesis
Presented to
the Graduate School of
Clemson University

In Partial Fulfillment
of the Requirements for the Degree
Master of Science
Physics

---

by
Matthew Preston Ray
December 2006

Accepted by:
Dr. Chad E. Sosolik, Committee Chair
Dr. Chad E. Sosolik
Dr. Joseph R. Manson
Dr. Terry M. Tritt

ABSTRACT

A hyperthermal and low energy ion beamline to measure electron-hole pair production due to ion bombardment of Schottky diodes has been modified and assembled.

A brief overview of the instrument is given and the reason for operating the ion beamline in the hyperthermal and low energy regime is discussed. The capabilities of the ion beamline are unique and provide the means to measure quantities that offer insight into various energy exchange mechanisms that occur at surfaces. Combined with the ability to accept Schottky diode samples, the beamline is capable of measuring both charge transfer and electron-hole pair production caused by ion bombardment of the sample.

Details of assembly and modification of the ion beamline as well as theory of operation are discussed. Data verifying the precision of the beamline mass and charge selection processes is provided along with a profile of the ion beam. The beamline has been upgraded to enhance reliability by replacing diffusion pumps with turbomolecular vacuum pumps. Also, the scattering chamber has been outfitted with a load lock system to drastically reduce sample turnaround time, an important feature for the Schottky diode experiments.

The theory of Schottky barriers and Schottky diodes is also discussed. Current and voltage measurements were taken on the Schottky diode device and were used to calculate the Schottky barrier height. Using an Ar^+ high flux ion beam and Na^+ low flux ion beam, preliminary electron hole pair measurements on a Schottky diode are presented. A possible explanation of results is provided by considering an analogue to Schottky diodes, metal-insulator-metal tunnel junctions [1].

ACKNOWLEDGEMENTS

I would like to thank my advisor, Dr. Chad Sosolik, for his guidance over the past two and a half years. He has taught me practically everything I know about surface physics and without his insight, this thesis would not have been possible. His patience and dedication has been an inspiration.

I am also grateful for the suggestions and time of my committee members Dr. Joseph Manson and Dr. Terry Tritt.

My parents also deserve acknowledgment. Without their support, my time at Clemson would have been miserable and I certainly wouldn't have made it this far.

I also appreciate my fellow lab members, especially Stephen Moody and Russell Lake.

TABLE OF CONTENTS

Table of Contents (Continued)

LIST OF TABLES

LIST OF FIGURES

List of Figures (Continued)

CHAPTER ONE
INTRODUCTION

The ion beamline at Clemson University is a tool for studying energy exchange mechanisms at surfaces. The ion beamline operates at low and hyperthermal energies where the scattering of ions off the sample is most probable. The beamline is held under ultra high vacuum (UHV) and is separated into three sections: the ion source section, the monochromator section and the scattering chamber. A beam of ions is formed in the ion source section, the beam is mass and charge selected in the monochromator section and finally, the beam is then passed into the scattering chamber where the beam scatters off of a sample. After scattering from the sample, the beam is collected by an electrostatic analyzer (ESA).

The surface is probed indirectly by scattering the ion beam off the sample surface into the ESA detector where variations in the scattered ion energy are measured. The energy measured by the ESA gives the total loss of ion energy to the surface. Direct measurement of the different components that make up the total energy loss at the surface cannot be measured by the ESA. However, recent studies use Schottky diodes to show that electron-hole pairs can be measured as a "chemicurrent" [2,3]. Electron-hole pair production is one of many energy exchange mechanisms that surfaces use to absorb energy. That is to say, Schottky diodes offer a way to directly probe the energy associated with e-h pair production which is a component of the total energy imparted to the surface measured by the ESA.

Previous studies measuring e-h pair production using Schottky diodes have been limited to neutral, thermal energy beams[2,3]. The ion beamline at Clemson University offers a way

to extend previous measurements to the hyperthermal and low energy regime and uses a wide range of source species. Experiments varying the beam energy and source species have not been conducted to date. The unique capabilities of the ion beamline at Clemson University make it the ideal instrument for carrying out these experiments.

The ion beamline was assembled and existing components of the beamline apparatus were modified to accept the Schottky diode samples. The details of assembly, modification, as well as, preliminary data on a Cr Schottky diode are presented in this thesis.

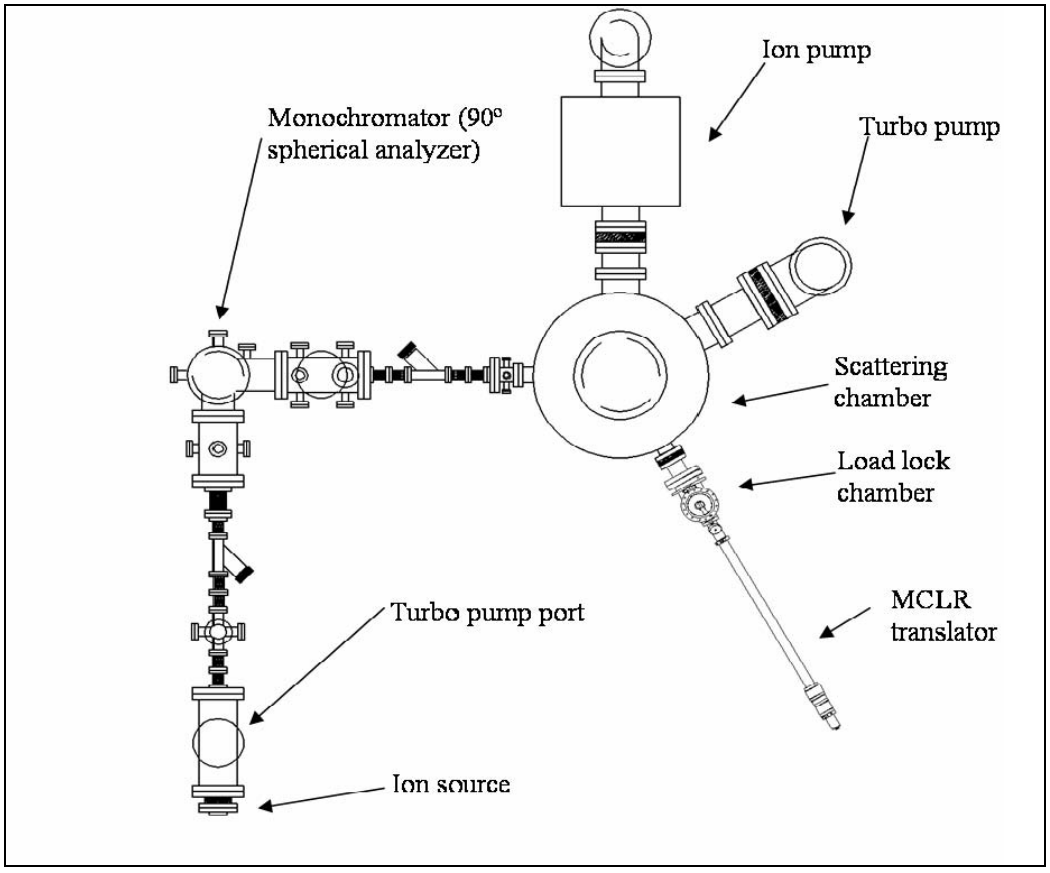

Figure 1.1 Plan view of the ion beamline. The magnetically coupled linear-rotary (MCLR) translator and load lock were two additions to the beamline. The load lock and MCLR translator facilitate Schottky diode sample exchange without breaking vacuum and drastically reduce sample turnaround time.

CHAPTER TWO
ASSEMBLY AND MODIFICATION OF THE LOW AND HYPERTHERMAL ENERGY BEAMLINE

Introduction

The low and hyperthermal energy beamline is a tool for measuring surface scattering spectroscopies. The beamline is made of three main sections: the source, monochromator and scattering chamber. The source section is made up of a G-2 Ion Gun manufactured by Colutron Research Corporation[4]. The monochromator section was built using readily available vacuum hardware. The scattering chamber was designed by students and manufactured by Perkin-Elmer Vacuum Products. All three sections are under Ultra High Vacuum (UHV). Originally constructed at Cornell University [5] in 1987, the ion beamline was moved to Clemson University in the spring of 2004. At Cornell University, the instrument was used to study the kinematics of ion-surface collisions. Various specifications, which I will discuss at length later in this chapter, were required for the instrument to collect data accurately and reliably for these experiments. While the operating characteristics have not been changed, the beamline has been updated to allow the system to be more user-friendly, efficient and more reliable.

Beamline Characteristics

As mentioned previously, the ion beamline operates in the hyperthermal and low energy regimes. The hyperthemal energy regime is defined roughly as energies above thermal (<1 eV) but less than 1 keV. The low energy regime is defined as energies between 1 keV and

10 keV. The ion beam is operated in the hyperthermal and low energy regimes because the scattering probability is maximized. As Figure 2.1 shows, ions with energy below the hyperthermal regime are typically adsorbed on the surface. Ions with energy higher than the low energy regime are implanted into the sample. This is important because if the ion is not scattered off the sample, any interaction information is lost because the ion is not detected after the interaction.

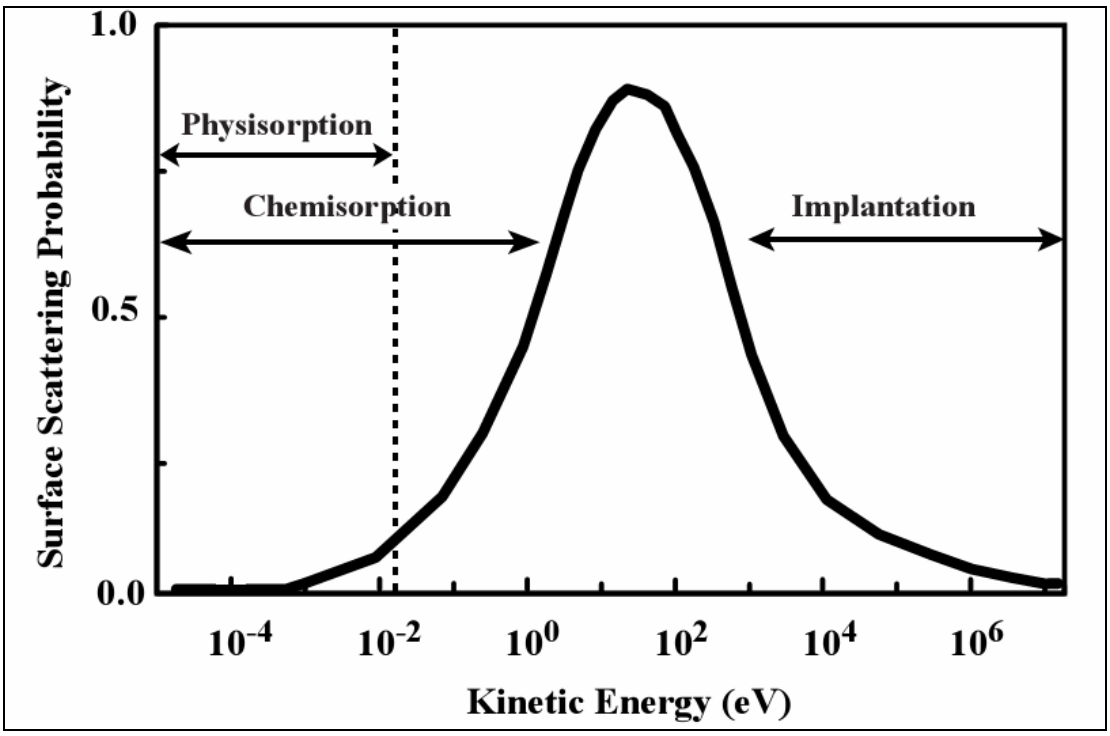

Figure 2.1 Graph of the kinetic energy regimes for single-particle scattering event. Note that the scattering probability is peaked in the hyperthermal energy regime.

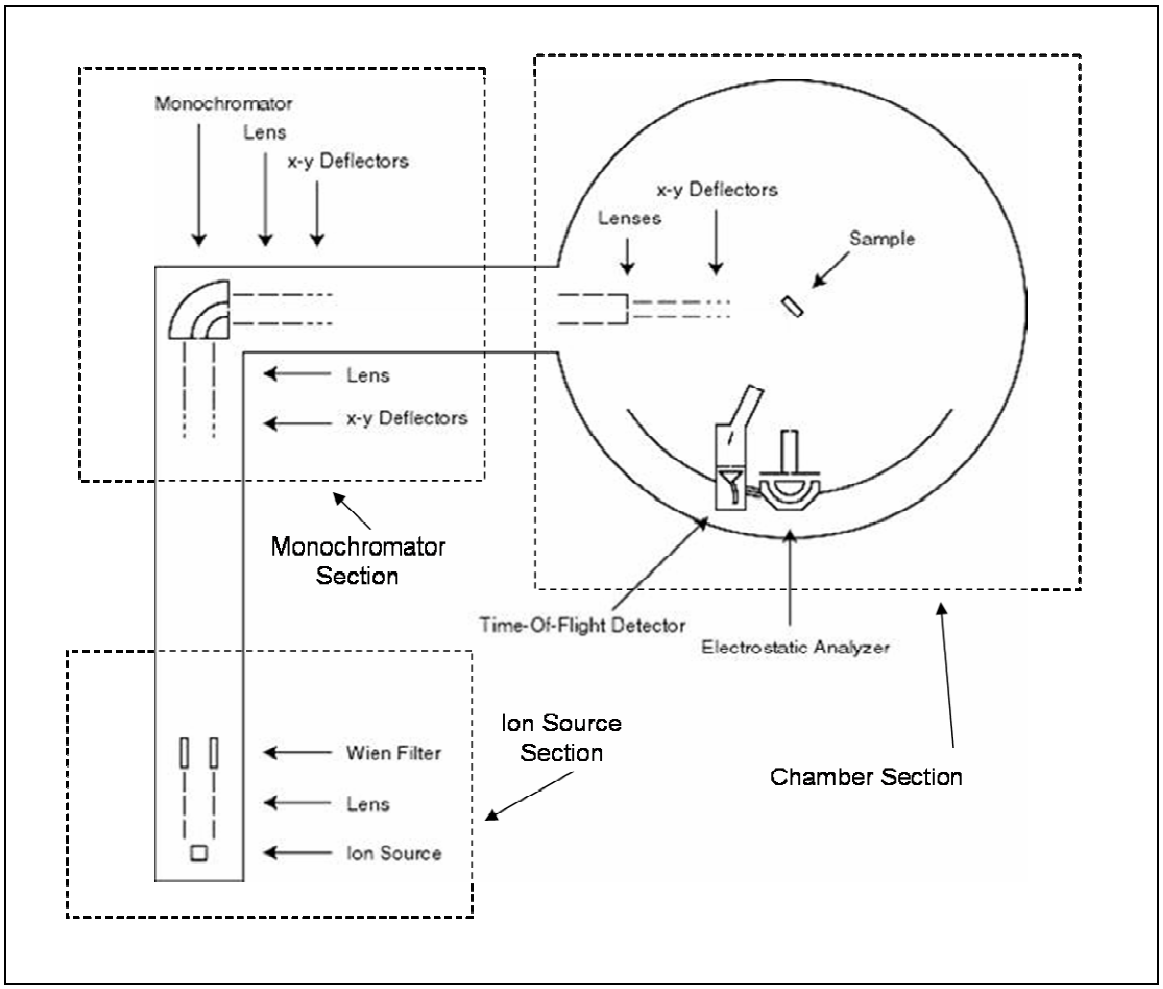

Figure 2.2 Schematic view of the beamline. This shows the three sections that comprise the ion beamline.

The Source Section

The entire beamline operates at UHV and uses either gas or alkali sources. The source section is made up primarily of the G-2 ion gun. The G-2 ion gun contains the gas or alkali source and the Wein filter [4]. Floating the sources at voltage relative to the target provides the beam energy. The gas sources use a hot filament to thermally ionize the incoming gas. The alkali sources rely on heating an aluminosilicate compound that contains the alkali atom. The aluminosilcate compound is melted into a porous tungsten plug. The porous tungsten

contains the alumiosilicate but also allows emission to occur. Heating the alumiosilicate imparts enough energy to free the alkali atom. Properties of the aluiminosilicate lattice cause the ionization the alkali atom. Once free from the aluminosilicate lattice, the alkali ions are accelerated away from the source by a applying a small bias voltage between the source filament and source body. The alkali sources are purchased from Heatwaves Labs Incorporated[6].

After the atoms are ionized, they pass into a Wein filter where the ions are selected by their charge to mass ratio. A Wein filter consists of orthogonal electric and magnetic fields. To create the magnetic field for the Wein filter, the G-2 ion gun uses an electromagnet. Passing a current through the electromagnet produces a magnetic field. Using a LabView program, the magnet current is varied and a relative mass spectrum is produced by plotting the current provided to the electromagnet versus the electrometer reading off the source section Faraday cup. The magnet current is capable of being swept as high as 20 A. According to Colutron Research Corporation, the manufacturer of the G-2 ion gun [4], the magnetic field produced and the current provided to the electromagnet are linearly proportional. In order to calculate the relative masses, the Lorentz force law applies:

$$\mathbf{F} = q(\mathbf{E} + \mathbf{v} \times \mathbf{B}) \tag{1}$$

Because the force on a mass passing through the Wein filter is zero and the velocity and magnetic field are orthogonal, the following equation is true:

$$\frac{-E}{B} = v \tag{2}$$

Also, the kinetic energy is defined as:

$$\frac{1}{2} mv^2 = \text{K.E.} \tag{3}$$

Using the equations (2) and (3), the following equation can be obtained:

$$\left[\frac{-E}{B}\right]^2 = 2\,\frac{K.E.}{m} \tag{4}$$

Throughout an experiment the energy of the ions is fixed by the voltage V specified by the user. The kinetic energy of a charged particle is:

$$\text{K.E.} = qV \tag{5}$$

The ions are assumed to be singly charged hence the energy of a single ion is:

$$\text{K.E.} = e^{+}V \tag{6}$$

Also, the electric field remains fixed during a sweep of the magnetic field. Dividing equation (4) by itself for differing magnetic fields corresponding to different masses, one obtains the following:

$$\left[\frac{B_2}{B_1}\right]^2 = \frac{m_2}{m_1} \tag{7}$$

This equation allows the B-field to be rescaled for mass. If the largest peak in the spectrum is assumed to be the mass of the source species, then one can create a relative mass spectrum by knowing the mass of the source species. Figure 2.3 shows a graph of intensity versus mass. The intensity is beam current measured in the source section Faraday cup as the magnet current is varied divided by the maximum beam current measured by the source section Faraday cup. The maximum beam current measured by the source section Faraday cup is assumed to be associated with the source species.

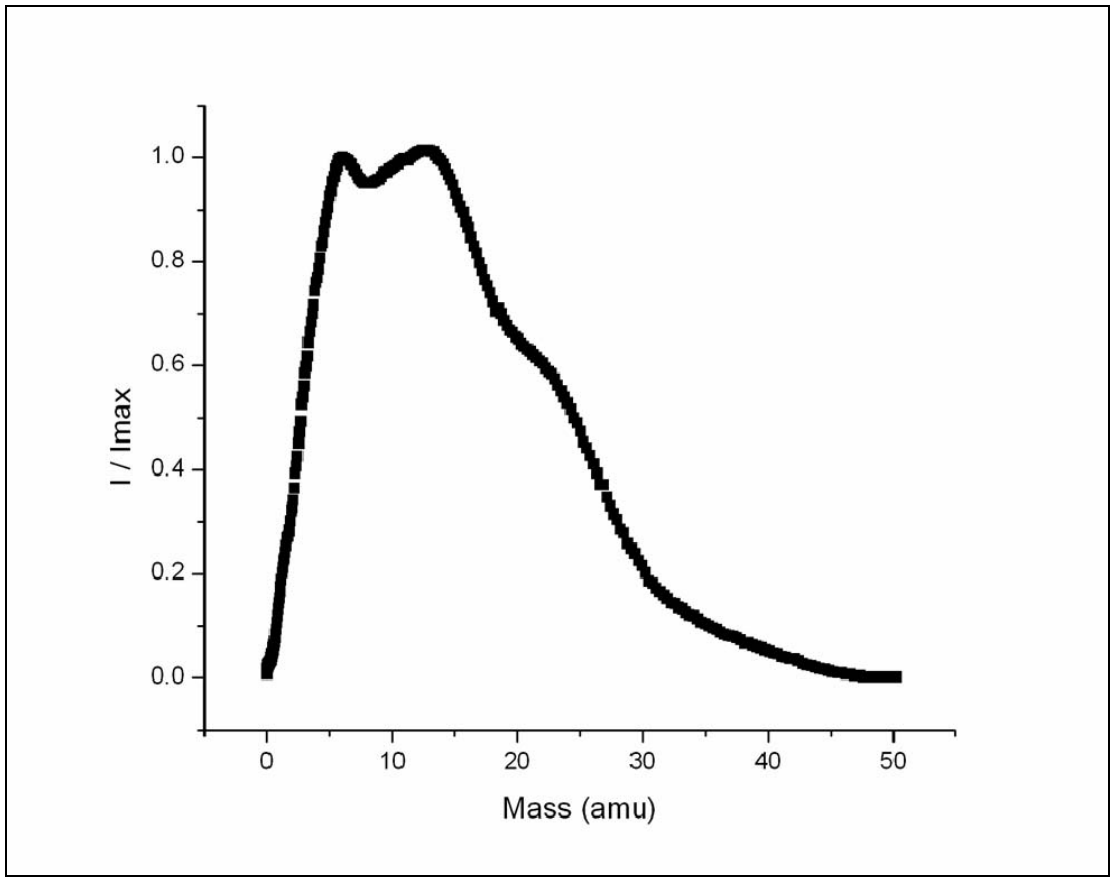

Figure 2.3 Sample Li7 mass spectrum. There are many peaks in this spectrum because the source was new. Impurities associated with the manufacture of the alkali sources cause several peaks in the spectrum. As the alkali source runs for several hours, the impurity peaks disappear leaving a dominant peak associated with the source specie.

The Monochromator Section

After the ions have been mass selected by the Wein filter, the ions are energy selected by the monochromator. When the beam energy is set by floating the source to voltage, the beam energy may be offset due to thermal variations and biasing within the source. The monochromator is in essence a spherical electrostatic analyzer designed to energy resolve the beam with a precision of $\frac{\Delta E}{E} \approx$ 1% [7]. Unfortunately, the monochromator was damaged in shipment to Clemson. The insulator isolating the outer sphere of the monochromator

from the vacuum housing had broken. This problem was resolved by removing the insulator and bolt which held the monochromator to the vacuum housing. Removing the bolt had no operational effect on the monochomator. However, it should be noted that the monochromator is simply resting on sapphire insulators and is not rigidly attached to the vacuum housing. In order to remove the broken insulator, the entire monochromator was disassembled. While disassembled, the internal wiring and pinouts were carefully documented. (see Appendix A)

The Chamber Section

After the ion beam has been mass selected by the Wein filter and energy resolved by the monochromator, the beam is passed into the scattering chamber. Once scattered off of the sample, the ions are detected by an electrostatic analyzer (ESA). The ESA rests on a rotatable table. Depending on the scattering angle of the ions, the ESA can be rotated to a scattering angle up to 130°. Rotating the table under UHV is made possible by attaching the table driveshaft to a differentially pumped rotating seal. Using a Vernier type scale on the rotating flange, the angles are reproducibly accurate to within ±0.2°[8]. However, because the sample does not rotate about the center of the scattering chamber, the Y-axis micrometer on the manipulator must be adjusted to compensate for the off-center rotation [9].

The ESA is an 180° spherical electrostatic analyzer with a Channeltron electron multiplier (Galileo Electron-Optics Model 4816) at the output [10]. The spheres of the analyzer have a mean radius of 50 mm. The ESA measures scattered ion energy by only allowing ions of a particular energy to pass to the detector. Once through the analyzer, the

ions are accelerated into the multiplier by biasing the multiplier at high voltage. This voltage can be tuned to provide peak efficiency. A bias of 2400 V seems to be most efficient for the current setup. The multiplier is connected to preamp discriminator (MIT F100-T). The preamp provides TTL pulses which are fed to a Hewlett-Packard 5335A counter [11]. The counter is connected to a computer with a GPIB card and a LabView® program automates scanning the ESA and also produces the energy spectrum. The ESA is scanned through a range of energies by changing the hemisphere voltages to produce an energy spectrum. The precision of the ESA is approximately 1%. Figure 2.4 shows a sample energy spectrum of the incident beam.

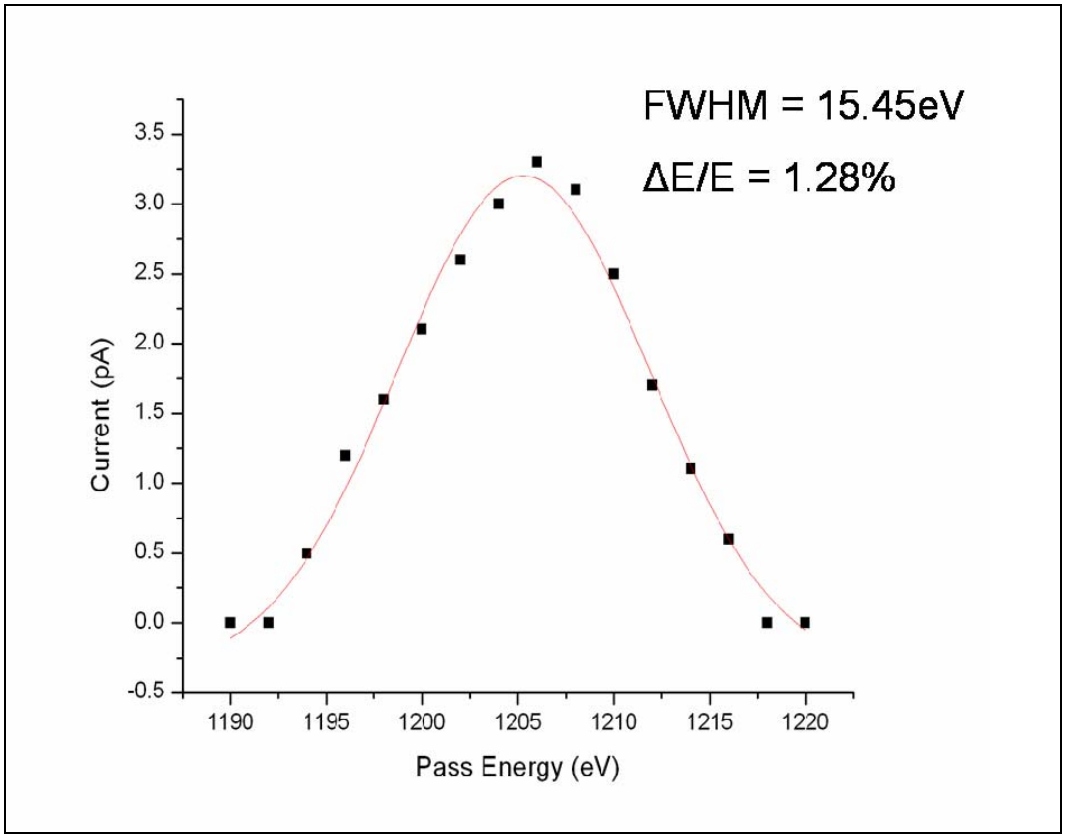

Figure 2.4 ESA spectrum. This is an ESA energy spectrum of a 1205 eV Na^+ beam. Note that this spectrum is not a scattered spectrum, but a spectrum verifying the precision of the monochromator.

Once in the scattering chamber, the ion beam is measured using a Keithley 617 electrometer [12]. The current on the sample is maximized by varying parameters mentioned previously. In order to measure the beam profile, a specialized Faraday cup has been placed on the end of the manipulator. The cup consists of a faceplate with a 1 mm aperture, an oxygen-free, high-conductivity (OFHC) copper current trap and a shield. There is also a 1 mm aperture between the faceplate and the current trap. The aperture is electrically isolated from the faceplate and the current trap. The aperture can be negatively biased to prevent secondary electrons at the faceplate from reaching the trap. Also, the trap itself can be biased slightly positively in order to keep secondary electrons created from escaping. These secondary electrons are created from the ion impact events. The shield protects the backside of the Faraday cup from stray ions and electrons inside the chamber [13].

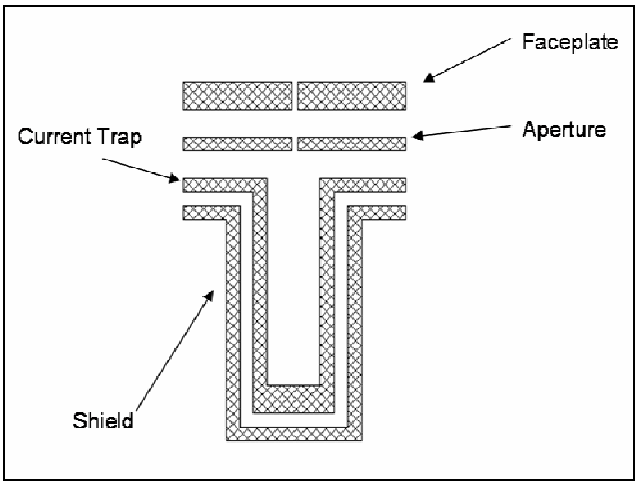

Figure 2.5 Cross sectional view of chamber Faraday cup [14].

In order to create a profile of the ion beam, the chamber Faraday cup was translated in the plane perpendicular to the ion beam and current measurements were taken. Figure 2.6 shows a typical beam profile.

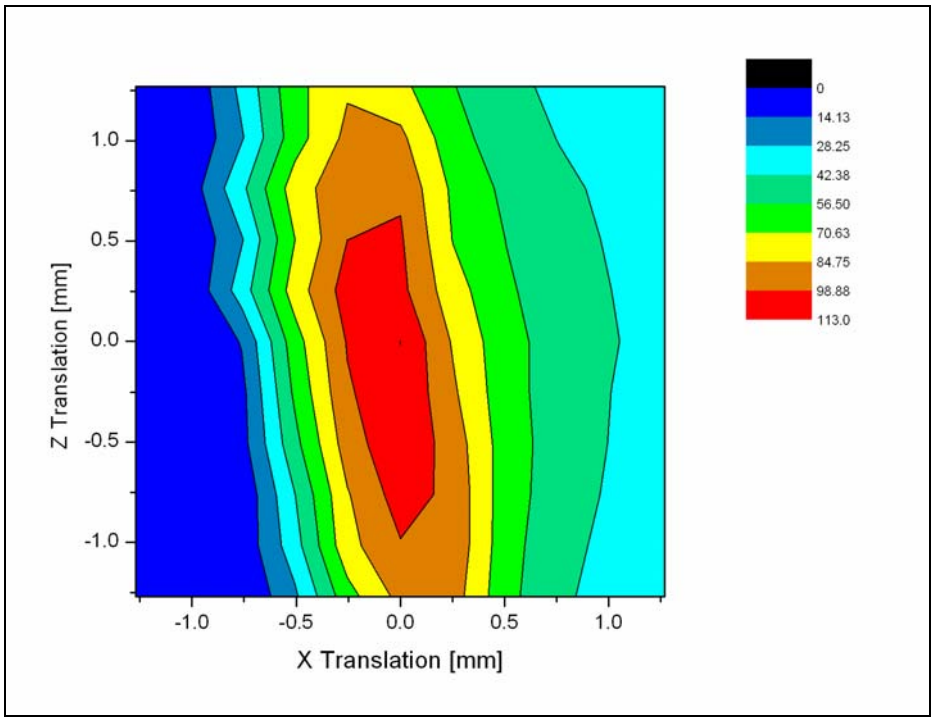

Figure 2.6 Beam profile of 1200 eV Rb^+ ion beam. The intensity is measured in pA.

Built buy Perkin-Elmer Vacuum Products, the scattering chamber possesses capabilities to fully characterize and prepare the sample. Instruments attached to the scattering chamber for sample characterization include: a sputter gun, LEED optics, Kelvin probe for work function measurements, Perkin-Elmer Auger spectrometer and a residual gas analyzer.

Also, the sample carrier has two modes for sample heating. The sample can be heated via radiation or electron beam heating. The heater is made of 0.004" W wire that is wrapped around a 0.030" drill bit [15]. Wrapping the wire around the drill bit produces a coiled heater filament. This coiled heater is mounted behind the sample and is also electrically isolated from the sample with Alumina washers. The radiation mode of heating is activated by passing a current through the heater filament, heating the filament. The hot filament

heats the sample by radiation. In the electron beam heating mode, a current is passed through the heater filament and the filament is biased at a voltage relative to the sample. The hot filament emits electrons which are accelerated by the voltage striking the backside of the sample. This electron bombardment causes the sample temperature to increase. The heater is mounted inside a tantalum shield that prevents evaporated tungsten from the hot heater filament from depositing onto the Alumina washers. This is an important detail because if the evaporated tungsten were to deposit on the insulating washers, a short would form between the sample and the heater filament. Should the filament break or a short develop, the heater is contained within the sample carrier which allows repair of the filament by transferring the sample carrier out of the chamber instead of venting the chamber.

The sample can be cooled to approximately 100K and heated to above 1073 K. Three flat copper braids connect the liquid nitrogen reservoir to the main body of the sample dock for cooling. A copper cooling head is attached to the main body, to provide efficient cooling of the sample. The cooling head is machined to accept the heat sink on the sample carrier. The temperature of the sample is monitored with an alumel-chromel thermocouple. The thermocouple is placed inside a 0.026" diameter hole drilled in the sample.

Ion Beam Transport Optics

The ion beam is transported at a minimum of 400eV in order to reduce space charge spreading of the beam [15]. Einzel lenses have been placed throughout the beamline as another measure taken to offset Coulombic repulsion of the ion beam. The first four lenses have an I.D. of 2.54cm. However, the fifth lens has an I.D. of 1.27cm. The focal properties scale with the lens diameter which allows the fifth lens to be placed closer to the sample.

The close proximity of the fifth lens to the sample reduces space charge spreading at the sample even further[16]. For experiments that require beam energy less than 400 eV, the fourth lens can decelerate the beam. However, for large deceleration ratios the fourth and fifth lenses are not well behaved. The fourth lens has a maximum deceleration ratio of approximately 40 [17]. For example, if the beam energy is 400 eV, then the fourth and fifth lenses can be used to decelerate the beam down to 10 eV.

At the end of each lens, there is an X-Y deflector. The deflector on each lens allows the beam to be steered. The deflector is important because between each section of the beamline there are pumping impedances. The pumping impedances have a 1mm aperture which the beam must pass through. The deflectors are used to steer the beam through these impedances. Figure 2.7 is a schematic view of the beamline. This figure shows the placement of the Einzel lenses, Wein filter, monochromator and ESA.

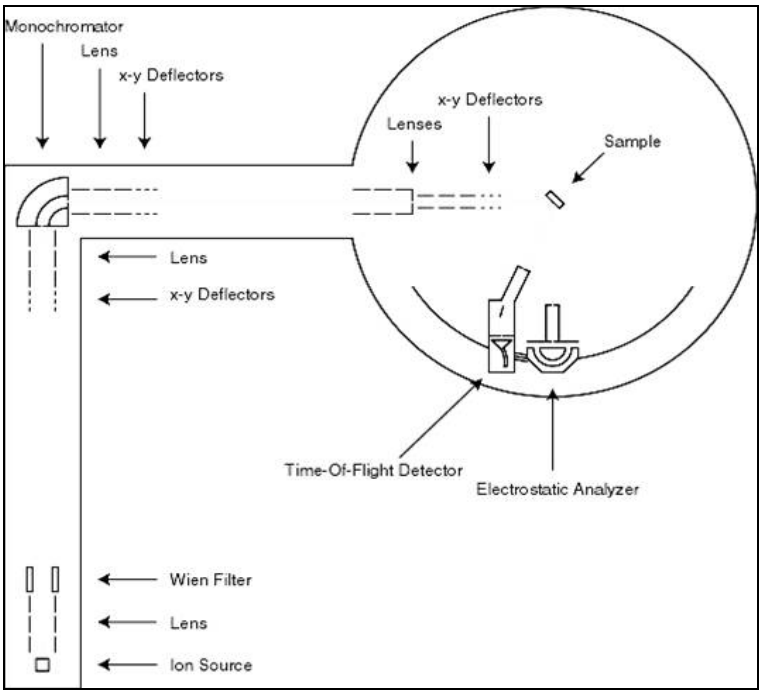

Figure 2.7 Schematic view of the ion beamline showing placement of Einzel lenses and deflectors.

Modifications to the Beamline

Several modifications were made to the beamline after being shipped to Clemson. A brief summary of modifications are:

- Shortened stands that support the beamline
- Replaced support stands on source and monochromator sections
- Replaced ion gauge controllers
- Incorporated interlock system into the source section of the beamline
- Replaced diffusion pumps with turbomolecular pumps
- Built pump coffins for mechanical backing pumps
- Installed sample transfer system on scattering chamber

The most noticeable change was shortening the stands that supported the beamline. The chamber support stand had to be shortened because the ceiling at Clemson was lower than at Cornell. Without shortening the legs of the support stand, the manipulator could not be removed from the chamber. The support stands for the source and monochromator sections of the beamline were replaced with a frame manufactured by 80-20 Corporation[18].

Two Varian multi-gauge controllers replaced the Granville-Phillips ion gauge controllers[19]. The Varian multi-gauge controlling the source section interfaces with an interlock system designed and built by the author. This interlock system is designed to controllably shut down the source section of the beamline in the event of power loss. The interlock uses a 24 VDC power supply and two 24 VDC relays to provide logic control of the system. If the building loses power, the interlock system will shut the gate valve between the vacuum pump and the source chamber, shut off the turbomolecular pump, close the foreline valve and the ion gauge will shut off. Once the interlock system has tripped, power will not come back to the turbomolecular pump, gate valve or foreline valve until the user resets the interlock. The interlock system prevents the vacuum components from cycling on and off should the building power cycle. Such a system will extend the life of the vacuum system components.

The Varian diffusion pumps originally on the source and chamber sections were replaced by Varian turbomolecular pumps. The pump on the source section is a Varian TV 301 that has a pumping speed of 280 l/s, while the chamber section has a Varian TV 551 with a pumping speed of 550 l/s. Replacing the diffusion pumps makes the beamline more reliable because the diffusion pumps required persistent maintenance in order to function properly.

Also, the liquid nitrogen needed for the cold caps on the diffusion pumps is no longer needed, thus reducing the lab's operating expenses. Both the Varian 500 l/s diode ion pump and the titanium sublimation pump from the old system maintain vacuum on the scattering chamber. Also, the cryopump originally on the monochromator section of the beamline has been omitted. The only pump on the monochromator section of the beamline is a Varian Model No. 911-5032 30 l/s ion pump.

Pump coffins were built for the mechanical backing pumps required for both the source and chamber turbomolecular pumps. The pump coffins were built out of plywood and lined with foam to reduce noise in the lab. The pump coffins were wired with fans and vented to provide cooling.

The scattering chamber has been outfitted with a sample transfer system. The sample transfer system allows a sample turnaround time on the order of days instead of weeks as previously required. The sample transfer system consists of two main components, the magnetically coupled linear-rotary translator (MCLRT) and the sample transfer head. The load lock has a hinged 6" viewport for sample loading. The MCLRT and load lock were manufactured by Thermionics Corporation[20]. The stainless steel sample transfer head is attached to the MCLRT shaft using a set screw and was machined by the Physics and Astronomy Machine Shop.

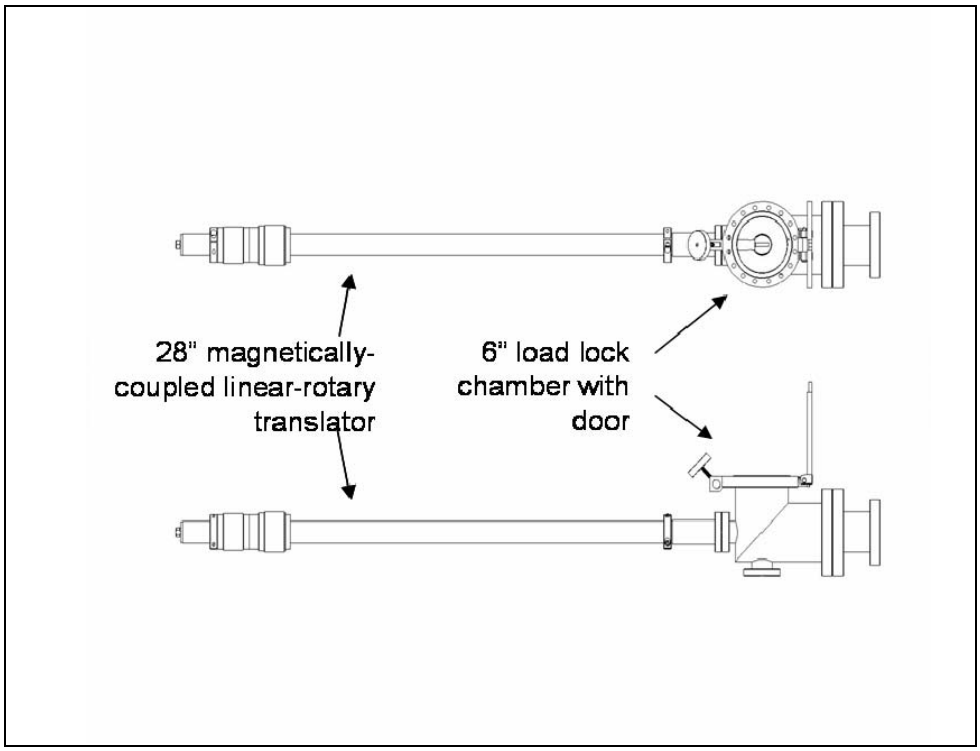

Figure 2.8 Sample transfer system. The MCLRT is attached to a 6" load lock chamber with a hinged viewport for sample loading. A 6" to 4.5" reducer is attached to the load lock chamber to allow the system to be mounted on an existing chamber viewport.

Not only was the load lock system added to the scattering chamber, the manipulator was retrofitted with a sample dock to accept the new sample carrier. The sample dock was designed by Stephen Moody and machined by the Clemson Physics and Astronomy Machine Shop. The sample carrier uses six transfer rings that provide both electrical and mechanical contacts to the sample dock.

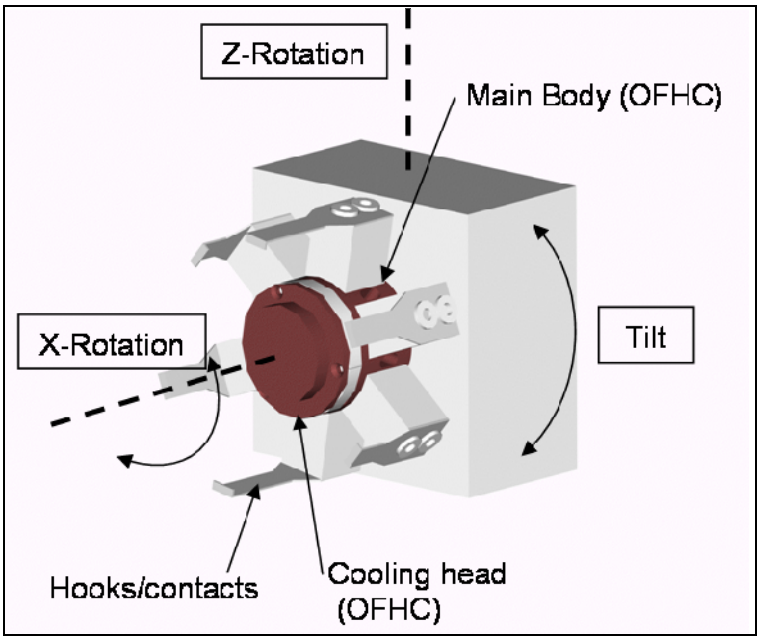

Figure 2.9 Sample dock. The sample dock has three degrees of freedom, X, Z and Tilt. The sample dock is mounted on the end of the manipulator. The cooling head and main body are made of OFHC copper.

The sample carrier provides 3 more electrical contacts than the previous design. The added electrical contacts are important to the Schottky diode experiment because they provide contacts for current measurement on the sample/metal layer, thermocouple leads, two leads for measuring current due to e-h pair creation, a lead to possibly bias the metal layer.

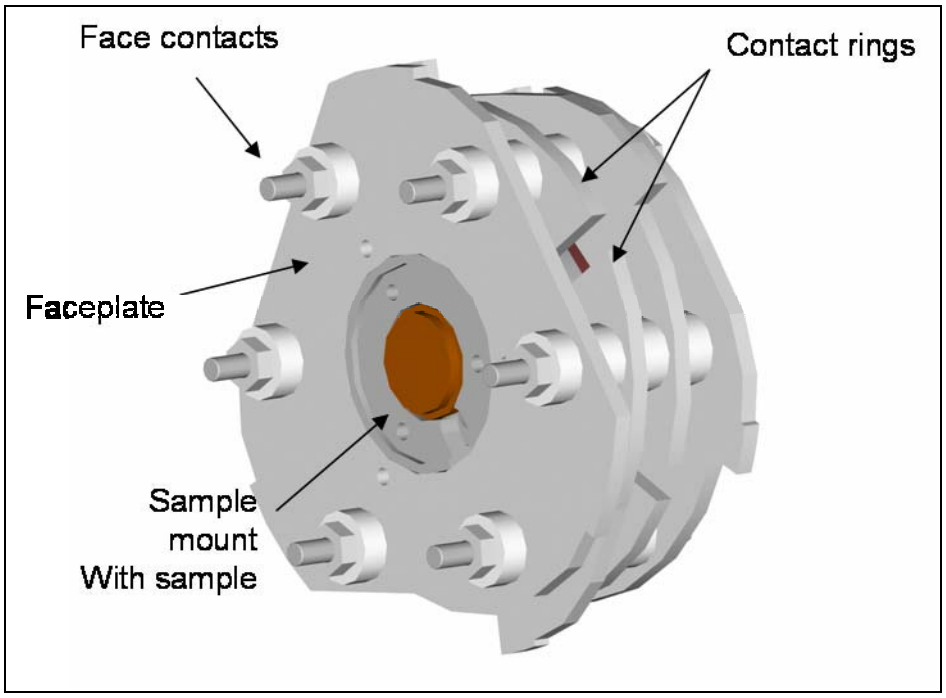

Figure 2.10 Sample Carrier showing sample, contact rings, faceplate and face contacts.

The faceplate of the sample carrier cam locks into the sample transfer head hooks. Once locked in position by the hooks, the sample carrier can be retracted or extended to or from the sample dock. Finally, the sample carrier is rotated clockwise or counterclockwise to either insert or remove the sample carrier from the sample dock.

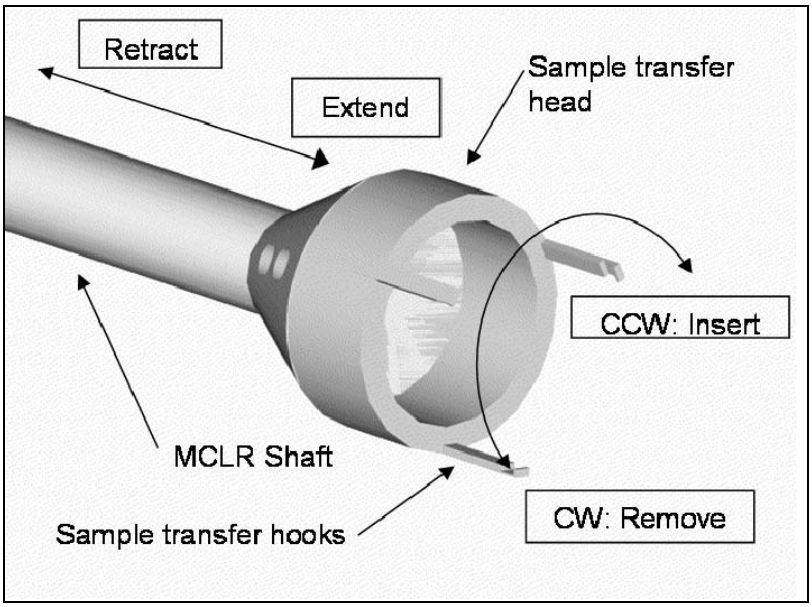

Figure 2.11 The sample transfer head. Mounted on the end of the MCLR, the sample transfer head holds the sample carrier while the MCLR transports the sample carrier between the load lock and sample dock.

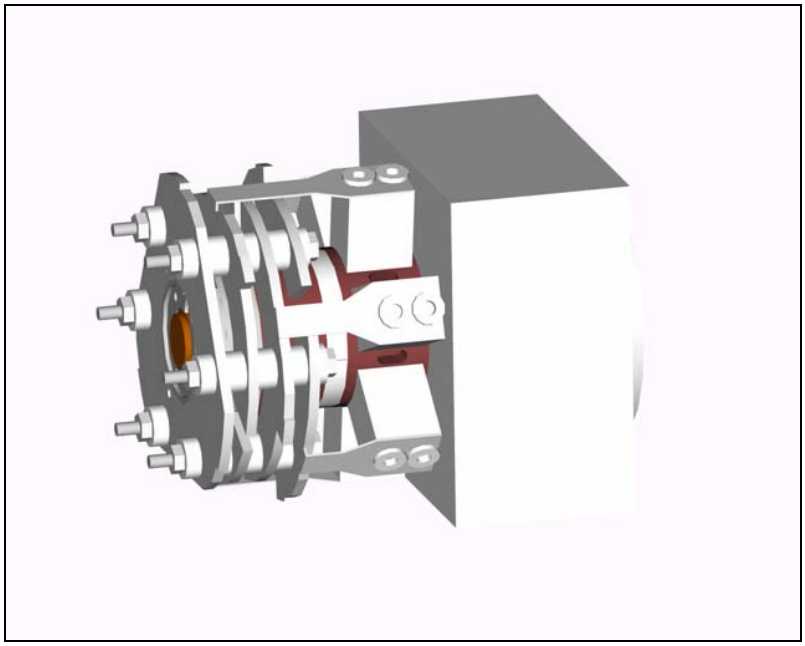

Figure 2.12 Sample carrier mounted in sample dock.

The load lock is vital to the Schottky diode experiments because the samples must be exchanged regularly to study how the metal layer thickness affects the chemicurrent.

LabView® code written by Stephen Moody interfaces with the Wein filter and Keithley electrometer to produce automated mass spectra. LabView® code was also written to control the Electrostatic Analyzer (ESA)[21]. The ESA code automatically produces energy spectra from scattering events. These LabView® programs make the beamline more user-friendly and allow efficient data acquisition.

CHAPTER THREE
SCHOTTKY DIODES

The ion beamline can accurately measure the total energy imparted to the surface using the ESA. However, measuring the energy exchange mechanisms within the surface is impossible using the setup mentioned previously. However, replacing the usual crystalline sample with a Schottky diode may offer insight into the electron-hole pair creation exchange mechanism caused by ion impact events. Experimentally, electron-hole pairs are difficult to detect. The recombination time of the electron-hole pair is small enough that detection is not possible. Only recent experiments using Schottky diodes by Neinhaus, et al. have electron-hole pairs been directly measured [2,3]. These experiments were carried out using thermal energy molecules. Having only thermal energy, the molecules are chemisorbed on the surface which imparts enough energy to the surface to create e-h pairs. However, there has not been any literature published to date that uses Schottky diodes to study electron-hole pair creation caused by ion impact events of hyperthermal and low energy. Since the ion beamline at Clemson operates most effectively in the hyperthermal and low energy regimes, it is the ideal instrument to take these measurements.

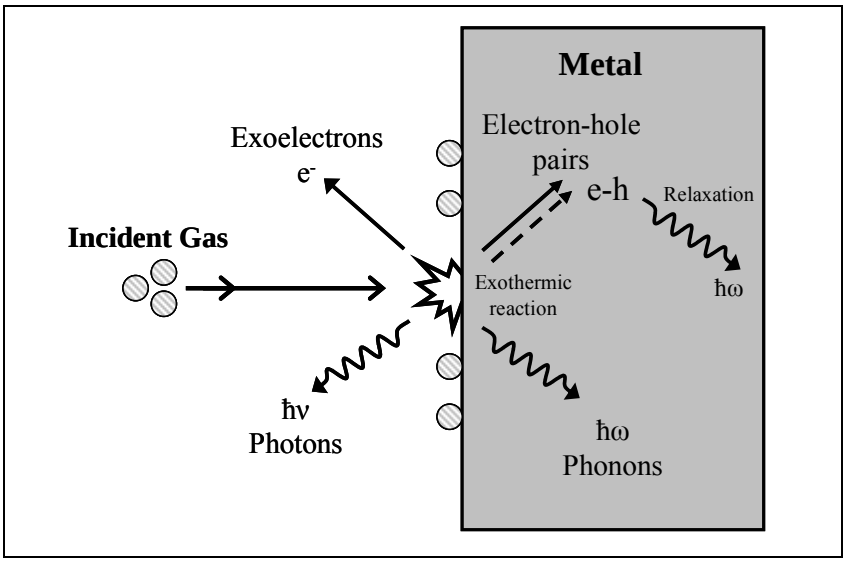

Figure 3.1 Depiction of different avenues of energy transfer [22].

The Schottky Barrier

The mechanism that makes a Schottky diode work is the Schottky barrier. The Schottky barrier is a rectifying barrier formed at the interface of a metal and a semiconductor. When a metal is brought into contact with a semiconductor, the Fermi levels of the metal and semiconductor do not match. The Fermi level in an n-type semiconductor is at a greater energy than the Fermi level of the metal. The difference in energy causes the electrons from the n-type semiconductor to traverse the metal-semiconductor interface and deposit into the more energetically favorable metal. However, the electrons leave positive ions in the semiconductor creating an excess of positive charge in the semiconductor, while creating an excess of negative charge in the metal. This separation of charges creates an electric field within the metal-semiconductor interface. The electrons that are depleted in the semiconductor are assumed to come from a finite layer within the semiconductor known as the depletion layer. This assumption is not exact but makes for a good approximation.

The total charge within the depletion layer is:

$$Q = N_d e x_d \tag{1}$$

where N_d is the donor concentration density, e is the charge of the electron and x_d is the depletion layer thickness. Applying Gauss's Law:

$$\frac{d}{dx}E = \frac{\rho}{\varepsilon} = \frac{N_d e}{\varepsilon} \tag{2}$$

Integrating for the electric field:

$$E(x) = \frac{N_d e}{\varepsilon}(x - x_d) \qquad \text{for } 0 < x < x_d \tag{3}$$

$$E(x) = 0 \qquad \text{for } x \geq x_d \tag{4}$$

The electric field for $x > x_d$ is assumed to be zero because the mobility of the charge carriers is such that the charge carriers can cancel any internal electric field. The electric field is the negative gradient of the potential. So, integrating the electric field and multiplying by -1 gives the potential:

$$\Phi(x) = \frac{N_d e}{2\varepsilon}\left[x_d{}^2 - (x - x_d)^2\right] \qquad \text{for } 0 < x < x_d \tag{6}$$

$$\Phi(x) = \frac{N_d e}{\varepsilon} x_d{}^2 \qquad \text{for } x \geq x_d \tag{7}$$

The energy shift due to the depletion layer is:

$$E_{shift} = e \cdot \Phi(x) \tag{8}$$

Applying equations (6), (7) and (8) [23] the energy bands within the semiconductor are shifted as:

$$E = E_{FB} - e \cdot \Phi(x) \tag{9}$$

where E_{FB} represents the energy from the flat band structures just after the metal and semiconductor make contact.

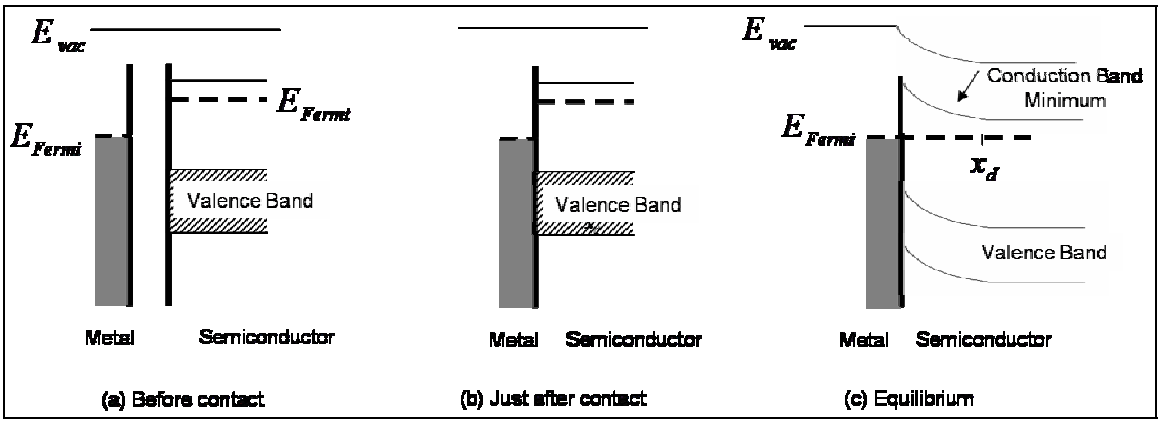

Figure 3.2 Energy Band Diagram for Schottky Diode. It is instructional, but not necessarily physically accurate, to consider the Schottky barrier in the following ways (a) before contact (b) just after contact but before any charges traverse the metal-semiconductor boundary (c) in thermal equilibrium after charges have traversed the boundary and bands of the semiconductor are bent [24]. This figure depicts band bending for an n-type semiconductor.

The Schottky diode

A Schottky diode consists of a thin metal layer deposited on a doped semiconductor. When an incident particle strikes the metal layer, energy is imparted to the surface which causes the production of electron-hole pairs. The electron from the metal lattice is excited above the Fermi level and leaves behind a hole in the conduction band of the metal. The excited electron, or "hot" electron, is ballistically transported across the barrier created by the metal-semiconductor interface. When the excited electron overcomes the Schottky

barrier, the electron-hole pair separate. The electron scatters, loses enough energy that it can't go back across the barrier to recombine with the hole.

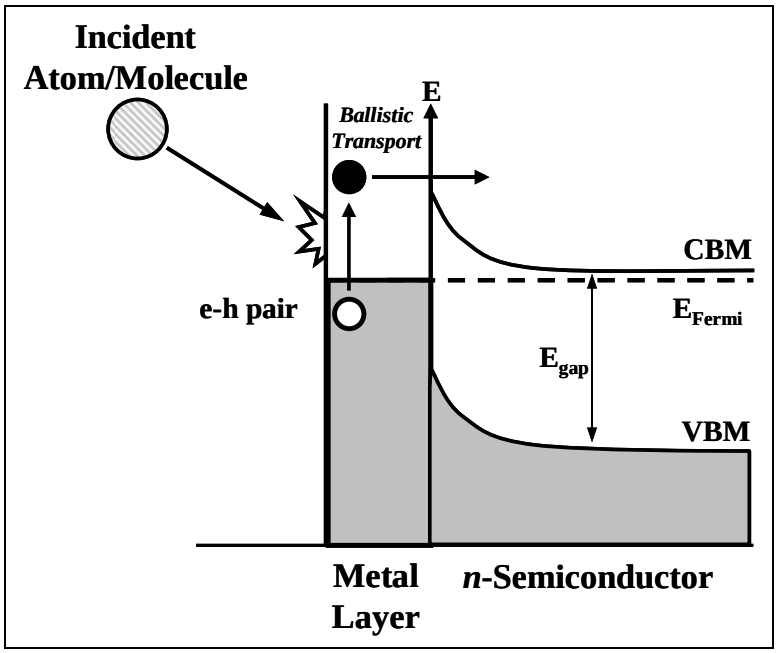

Figure 3.3 Depiction of e-h pair production in Schottky diode. After incident particle strikes the metal layer surface, electron hole pairs are created. The electron has enough energy to be ballisitically transported into the conduction band of the semiconductor [25].

Continually bombarding the metal layer with particles creates a bulk charge between the metal layer and the semiconductor. If an ammeter is placed across the barrier, the bulk charge flows through the circuit and is detected as a current.

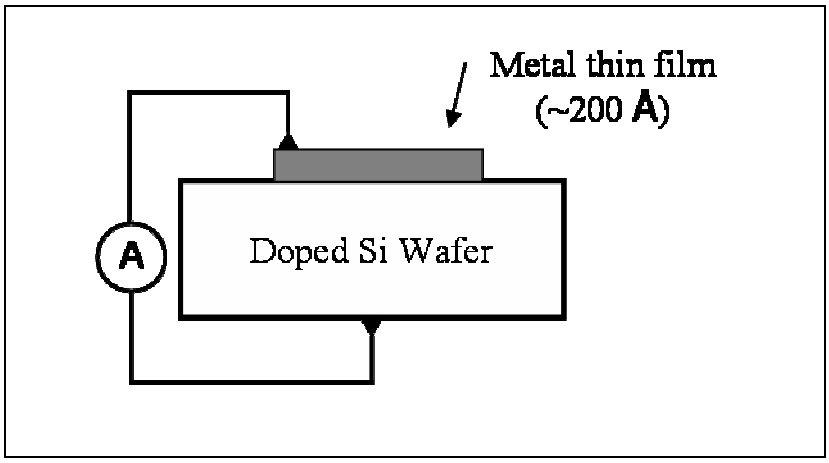

Figure 3.4 Wiring schematic for measuring current on a Schottky diode.

As one would expect, the current is strongly dependent on the thickness of the metal layer. When the metal layer thickness becomes greater than the mean free path of the electron, the current drops off rapidly [26].

Collaborating with Dr. Rod Harrell's group of the Clemson University Electrical Engineering Department, the Schottky diodes were manufactured in a clean room on campus. The Clemson University Engineering Department's clean room has all the equipment necessary to cut the substrate, anneal the backside contact, and evaporate the metal layer for the Schottky diodes. The first diode had a Cr metal layer that was 200Å thick and 1.25 cm in diameter. The metal layer and Al backside contact are all on a one inch diameter circular Si substrate. The backside contact was annealed to melt it into the Si substrate. Annealing makes the backside contact Ohmic. After the diode was made, the substrate was cut into the shape of a ¾" equilateral triangle to fit the physical constraints of the sample carrier.

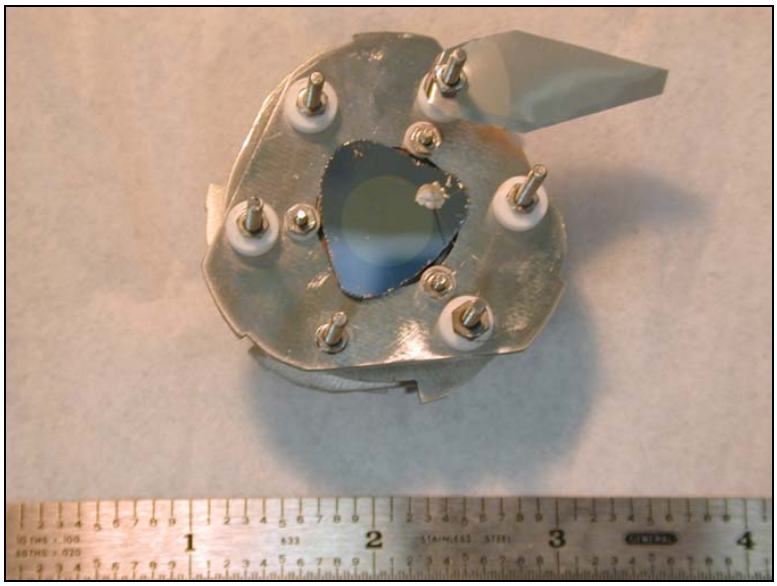

Figure 3.5 Mounted Schottky diode. This picture shows the triangular shape of the sample. The sample carrier constrains the shape of the diode. The metal shim acts to shield the bare wire connecting the metal layer from the ion beam. Note that the shield is not in place and has been moved such that the entire diode is viewable.

The electrical contacts to the sample dock were established through the sample carrier contact rings. However, because the physical dimensions of the Schottky diode were unknown at the time of sample carrier construction, the details of electrical connection to the diode itself were not determined. Knowing that some experiments would involve using metal crystal samples, the sample carrier faceplate was designed to hold these samples. While the faceplate worked well with the metal crystal samples, it put constraints on the physical dimensions of the Schottky diodes.

To mount the Schottky diode on the sample carrier, OFHC copper stock was machined to the dimensions of the metal crystal samples that are used for scattering experiments. The machined copper stock was used to adapt the Schottky diode to the sample carrier faceplate. The OFHC copper adaptor was installed just as a typical metal crystal sample. The OFHC

copper was chosen for its excellent electrical conductivity and was inexpensive compared to the metal crystal samples. This OFHC copper adaptor would provide the electrical contact to the backside contact of the Schottky diode. The diode was mechanically attached to the OFHC adaptor using product code H2OE silver epoxy manufactured by Epoxy Techonolgy[27]. The epoxy is applied to the backside contact of the Schottky diode and to the OFHC copper sample. Then the Schottky diode and OFHC copper sample are put together. The silver epoxy hardens over time forming a strong mechanical bond and is electrically conductive. The silver epoxy is also used to attach a wire to the metal layer of the diode forming the electrical contact to the metal layer. Thus, the backside contact and metal layer are connected to the sample carrier contact rings providing electrical contacts outside the vacuum chamber. A piece of 0.005" Ta shim was mounted on a faceplate contact to shield the wire contacting the metal layer to the sample carrier contact ring. If the shield were not in place, the ion beam could strike the wire creating a current that could be misconstrued as an energy exchange event.

After the silver epoxy is applied, the sample carrier was placed under a halogen lamp where the sample carrier is heated to 95° C for approximately three hours to fully cure the epoxy. The epoxy is vacuum compatible down to approximately 10^{-8} Torr according to the manufacturer.

Schottky Diode Characteristics

Schottky diodes are characterized by an ability to pass large amounts of current with a small voltage drop across the device. This characteristic makes the Schottky diode ideal for power supplies. A low voltage drop across the device means that only a minimal amount of power is lost through the diode, equating to more efficient power delivery.

The data presented henceforth was taken on the same Schottky diode mentioned previously with a 200Å thick Cr metal layer and n-type Si substrate. As one would anticipate, a measurement of current versus voltage is the most effective means of characterizing a Schottky diode. To take the current and voltage measurements, two leads of a Hewlett Packard model no. 4156B semiconductor parameter analyzer were connected to the diode. The HP-4156B semiconductor parameter analyzer belongs to Dr. Rod Harrell's research group in the Department of Electrical and Computer Engineering. The data presented in figures 3.6, 3.7 and 3.8 was taken by Michael Rodin of Dr. Rod Harrell's research group.

In order to take the I-V measurements, one lead is attached to the metal layer and the other connected to the backside contact. Varying the voltage between the metal layer and the backside contact, a current is sensed by the probes.

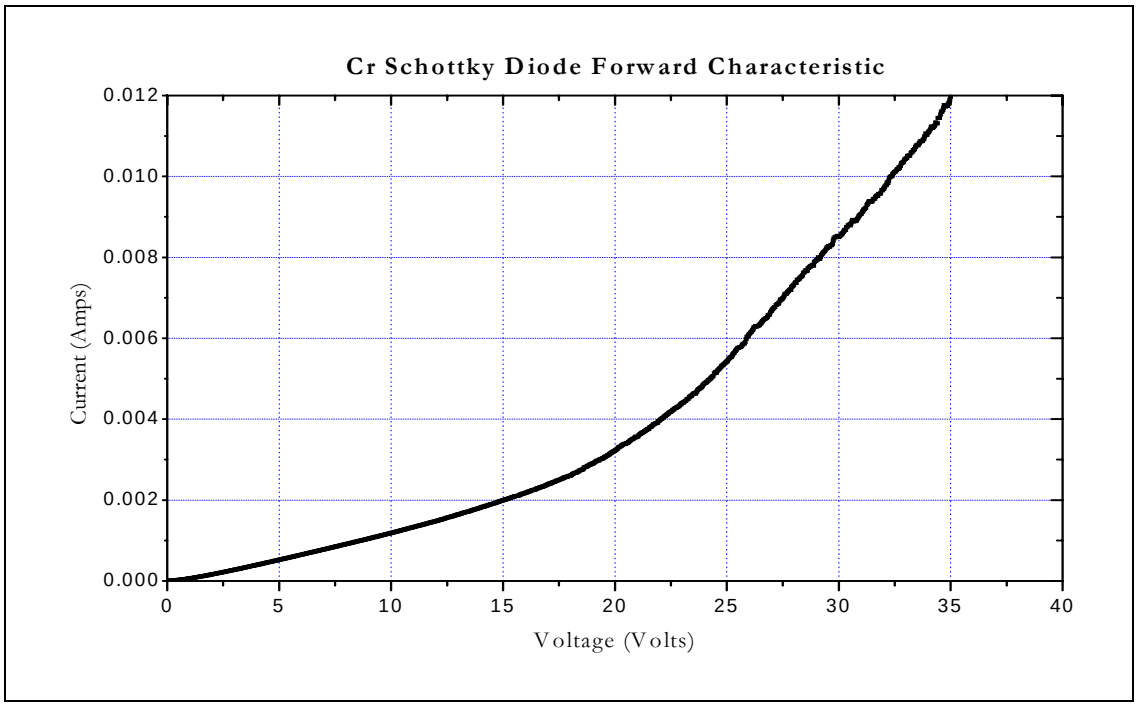

Figure 3.6 Data taken from Cr diode I-V measurements. The diode is forward biased meaning that the metal layer is taken to be the positive lead and the backside contact is the negative lead.

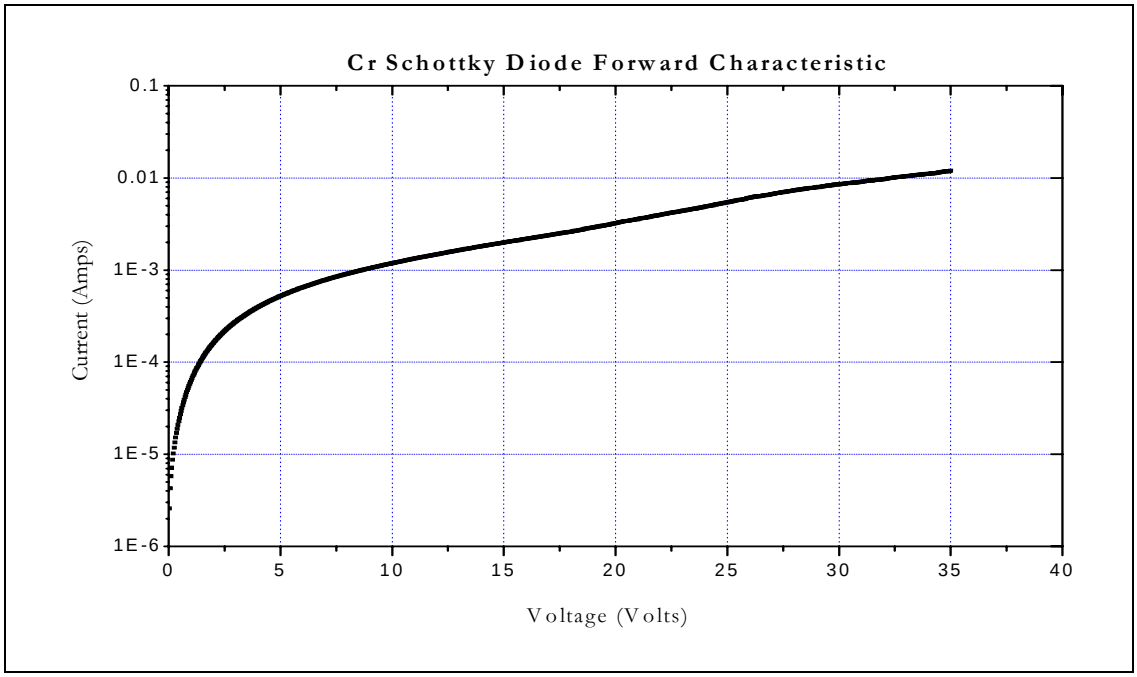

Figure 3.7 A graph of current versus voltage where the current is on a base ten logarithm scale. The data is the same as figure 3.6 and is also forward biased.

By applying a voltage across the diode, the height of the Schottky barrier is varied allowing more or less current to flow depending on the voltage bias. Current saturation occurs when all the charge carriers in the semiconductor are used to carry current to the metal layer. When the current and voltage become proportional on the graph of log current versus voltage the current is saturated. The saturation current density equation is shown below:

$$j_{ss} = A^{*}T^{2}e^{-\frac{\phi_b}{k_B T}} \tag{10}$$

Where j_{ss} is the saturation current density, A* is the Richardson constant, T is the temperature in Kelvin, ϕ_b is the Schottky barrier height, and k_B is Boltzmann's constant [22].

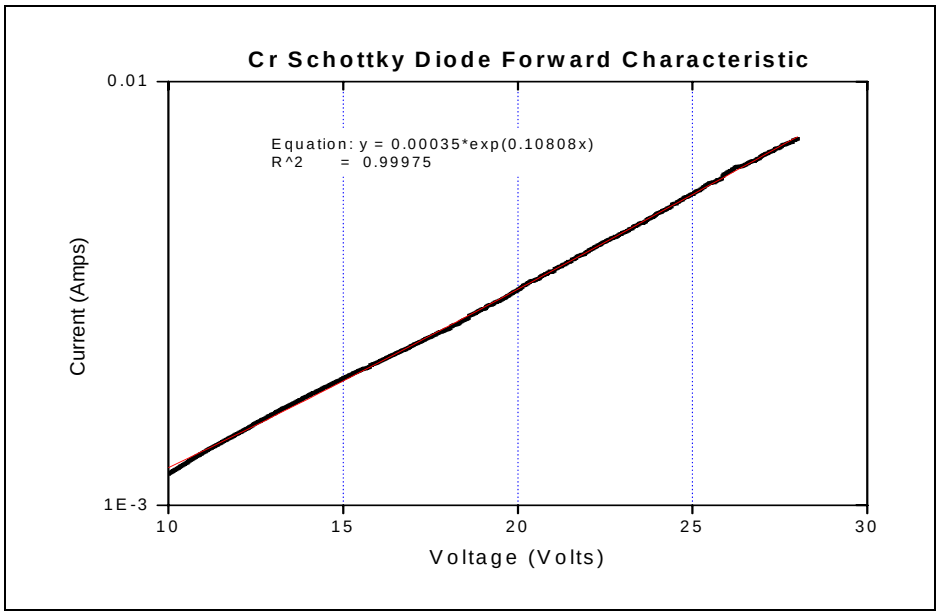

Figure 3.8 A graph showing the linear portion of figure 3.7. The constant first term in the best fit line equation represents the saturation current. Using equation (10) and the saturation current, the Schottky barrier height can be found.

The saturation current density is calculated by dividing the saturation current found in figure 3.8 by the area of the diode metal layer. After calculating the current density, equation (10) can be used to calculate the Schottky barrier height. Using a standard value of 120 $\frac{A}{cm^2 K^2}$ for the Richardson constant of Si and the saturation current density, the calculated value of the Schotkky barrier was 0.629 eV for the Cr metal layer Schottky diode.

The I-V measurements of the Cr metal layer diode show that it would not be a very effective diode for applications. The voltage required for the diode to pass current is quite high. This is probably due to a low concentration of charge carriers within the silicon substrate. However, the subject of interest is electron-hole pairs creating diode current, so the only parameter that is important to the experiment is the Schottky barrier height. In other words, the efficiency of the diode itself is inconsequential.

Diode Current due to Ion Bombardment

"Chemicurrent" is defined as the diode current caused by the chemisorption of particles onto the metal layer of the diode. The diode current due to e-h pair formation of this thesis is the equivalent to the "chemicurrent" measured in the thermal energy experiments performed by Nienhaus. However, the diode current shown in this thesis is most likely not due to chemisorption.

Schottky diode current measurements were made on the Cr metal layer diode. The measurements were taken with a Keithley 617 Electrometer. The diode was wired for current measurement just as in figure 3.4. The Cr metal layer of the diode was exposed to a beam of 1200 eV Na^+ ions and current was measured. The sudden current increase in

figure 3.9 could be due to surface contamination of the metal layer. The diode is prepared ex situ thus the diode is exposed to air after preparation. Exposure to air contaminates the surface of the Cr metal layer. This surface contamination would act to lower the work function of the metal layer. When the contaminated metal layer of the diode is exposed to the ion beam, electrons are excited out of the metal layer. These electrons can be excited over the Schottky barrier and measured as diode current. However, this current would die off as the surface contamination is sputtered away by the ion beam. This is a possible explanation for the intensity of figure 3.9.

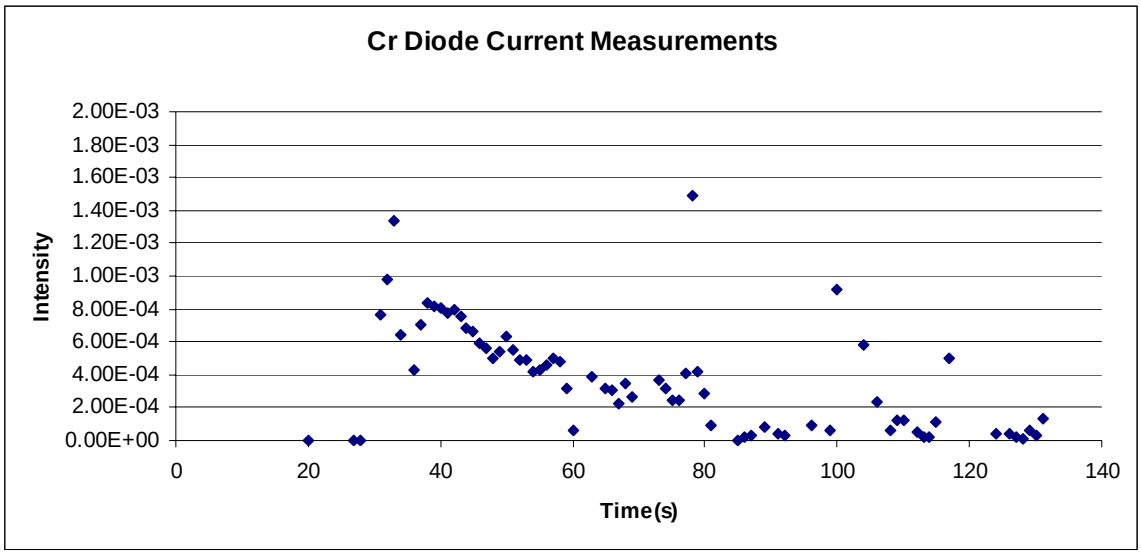

Figure 3.9 Plot of diode current intensity. The diode current is normalized to the beam current measured off of the chamber Faraday cup faceplate to form an intensity. The ion beam was Na^+ with energy 1200 eV. The Schottky diode is the same Cr metal layer diode which data was reported for in figures 3.6, 3.7 and 3.8. The diode was exposed at 30 s.

The beamline ion bombardment per second, or flux, is quite low making measurements that involve sputtering away the metal layer long measurements. Theoretically, the length of an experiment that would sputter away a 200 Å thick metal layer would last on the order of

days. This is not very practical as the beam current varies over such long periods of time. In order to take high flux measurements, the sputter gun on the scattering chamber was used.

The sputter beam current was approximately 3 orders of magnitude larger than for the Na^+ beam resulting in a higher flux of ions striking the diode surface. The sputter gun used an Ar^+ beam at 546 eV.

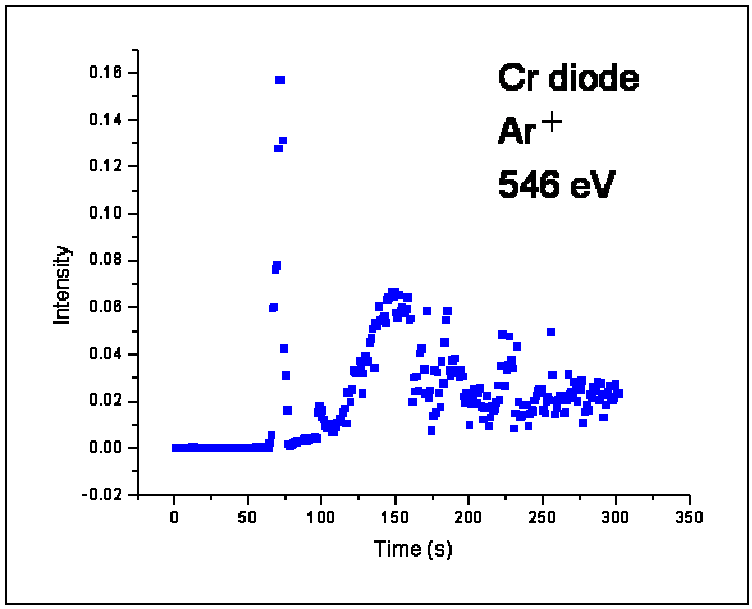

Figure 3.10 Graph of data taken using the sputter gun instead of the ion beamline. The sputter ion beam was 546 eV in energy and the source species was Ar^+. The diode was exposed at 60 s.

As in figure 3.9, figure 3.10 shows a strong peak when exposed to the ion beam. Again, this peak could be due to surface contamination. However, the second peak in figure 3.10 could be due to the sputtering away of the metal layer down to a thickness equal to the mean free path of the excited electron. This would allow the excited electrons to overcome the Schottky barrier and be measured as current. The noisy data shown in figure 3.10 after exposure times greater than 160 s may indicate destruction of the metal layer. A similar

trend to figure 3.10 is depicted by S. Meyer et. al. using metal-insulator-metal junctions instead of Schottky diodes[1].

Conclusion

In the future, more data should be taken to confirm the results of figure 3.10. Another issue to address is being able to produce a high flux of ions using the beamline in order to make more precise measurements. Although the sputter gun produces a high flux of ions, the sputter ion beam's energy and spatial extent is not as resolved as the beamline. Also, the beamline in not limited to gas sources like the sputter gun.

Also, measurements should be taken to find out how many electrons are leaving the metal layer of the Schottky diode due to ion impact. Electrons could leave the metal layer in two possible ways: electrons could leave by neutralization of the incoming ions and electrons could be expelled into the vacuum due to ion impact. A possible method for measuring the electrons leaving the metal layer would include shorting the metal layer to ground through an ammeter. Shorting the metal layer of the Schottky diode would provide the metal layer with a replenishment of electrons and prevent charge build up on the metal layer.

The low and hyperthermal energy ion beamline at Clemson University has been assembled, modified and is prepared for taking data on Schottky diodes.

APPENDIX

Appendix A

Monochromator Internal Wiring

Table A.1. Internal wiring table for the monochromator. There are two connectors that connect the internal wiring of the monochromator to outside of vacuum. The internal pins reflect values of the pins on the wiring breakout bar. The wires have metal tags that are attached to them. These metal tags have stamped numbers that associate them to various destinations. This table was formulated in June 2005.

Connector	Connector Pin	Internal Pin	Internal Tag	Destination
1	C	1	1	L1 Front Aperture, XY Rear Ring
1	D	2	2	XY1 Top
1	N	3	3	XY1 Left
1	P	4	4	XY1 Bottom
1	U	5	5	XY1 Right
1	E	6	6	L1 Element I
1	Q	-	-	Shield for Faraday Cup (Aluminum Can)
1	F	8	L1 Shield	L1 Element IV
2	2	9	9	L1 Element II
1	G	10	10	Screen Shield
2	1	11	11	L1 Element III
-	-	12	-	
2	4	13	12	MONO INNER SPHERE
1	R	7	faceplate	MONO FACEPLATES
2	5	15	15	MONO OUTER SPHERE
-	-	16	-	
2	3	17	17	L2 Element II
-	-	18	-	
2	6	19	19	L2 Element III
-	-	20	-	
-	-	21	-	
1	M	22	lens to shield	L2 Element I, Aperture, Shield
1	B	23	23	L2 Element IV
1	L	24	24	XY2 Right
1	A	25	25	XY2 Left
1	T	26	26	XY2 Bottom
1	K	27	27	L2 Exit and Entrance Rings
1	J	28	28	XY2 Top
1	H	NC		
1	S	NC		
1	V	NC		
2	7	NC		

Figure A.1 Figure of connectors 1 and 2 as well as a schematic depicting the destination of the wiring. Numbers and letters in parentheses correspond to the pins of connectors 1 and 2.

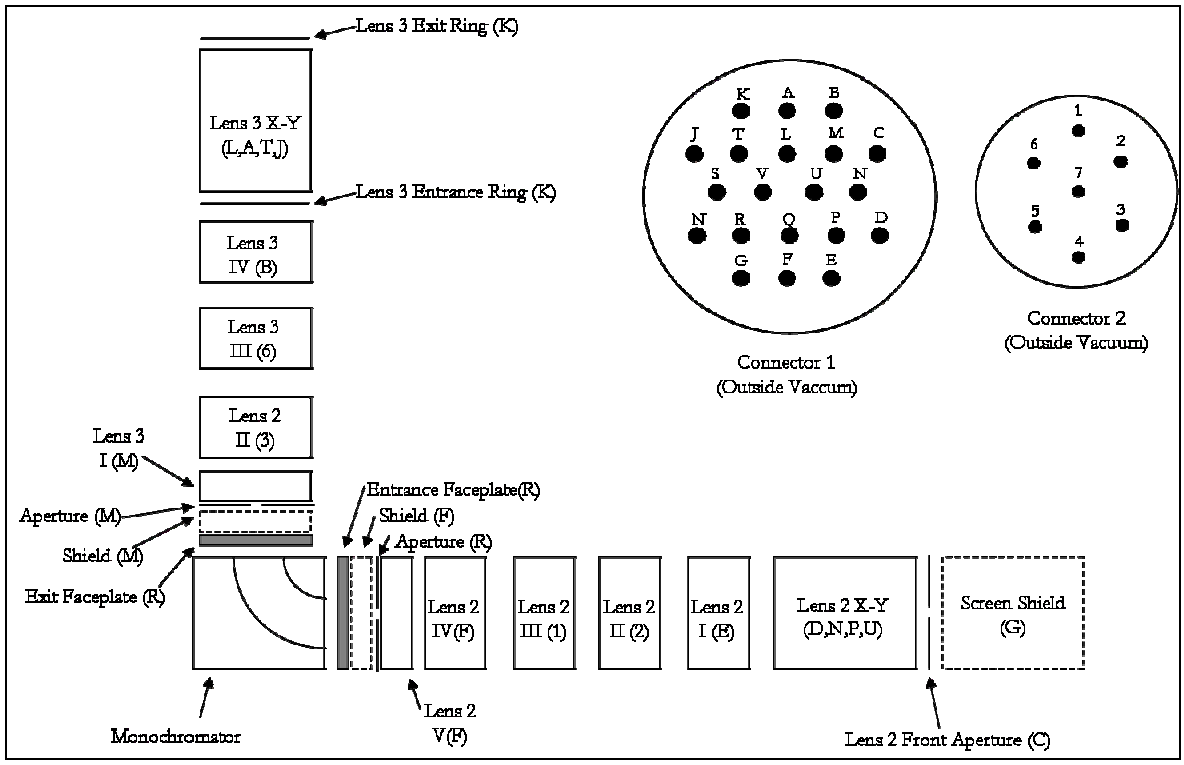

REFERENCES

1. S.Meyer et. al. *Nucl. Instr. And Meth. In Phys. Res. B* **230** 608-612 (2005)

2. H. Nienhaus *Phys. Rev. Lett.* **82** 446- 449 (1999).

3. H. Nienhaus *Appl. Phys. Lett.* **74** 4046-4048 (1999).

4. Colutron Research Corp., Boulder, CO 80301

5. D.L. Adler and B.H. Cooper, Rev. Sci. Instrum. **59**, 137 (1988)

6. Heatwave Labs, Inc., Watsonville, CA 95076

7. D. L. Adler *Kinematics of Hyperthermal Energy Ion Scattering* (Cornell University: Dissertation) (1989) 23.

8. R. L. McEachern *Trajectory and Impact Parameter Analysis of Hyperthermal Ion Scattering* (Cornell University: Dissertation) (1990) 29-30.

9. S. A.Moody Apparatus and Instrumentation Design for Hyperthermal- and Low- Energy Surface Impact Current Production (Clemson University: Thesis) (2006) 39.

10. McEachern 30.

11. Hewlett-Packard Company, Palo Alto, CA 94304

12. Keithley Instruments, Inc., Cleveland, OH 44139

13. Adler 30.

14. Adler 31.

15. McEachern 28.

16. Adler 29-30.

17. Adler 22.

18. 80/20, Inc., Columbia City, IN 46725

19. Varian, Inc., Palo Alto, CA 94304

20. Thermionics Vacuum Products, Port Townsend, WA 98368

21. Moody 32-36.

22. Adapted from H. Nienhaus *Surf. Sci. Rep.* **45** 5 (2002).

23. http://www.mtmi.vu.lt/pfk/funkc_dariniai/diod/schottky.htm

24. C. Kittel *Introduction to Solid State Physics* (J. Wiley and Sons) (2005) 507.

25. Adapted from H. Nienhaus *Phys. Rev. Lett.* **82** 446 (1999).

26. H. Nienhaus *Phys. Rev. Lett.* **82** 446 (1999).

27. Epoxy Technology, Billerica, MA 01821